



Design of automated system for online inspection using the convolutional neural network (CNN) technique in the image processing approach

Ha Quang Thinh Ngo ^{a,b,1}

^a Department of Mechatronics, Faculty of Mechanical Engineering, Ho Chi Minh City University of Technology (HCMUT), 268 Ly Thuong Kiet Street, District 10, Ho Chi Minh, Viet Nam

^b Vietnam National University-Ho Chi Minh City (VNU-HCM), Linh Trung Ward, Thu Duc City, Ho Chi Minh, Viet Nam

ARTICLE INFO

Keywords:

Inspection system
Visual technique
Computational mechanics

ABSTRACT

Presently, many achievements in various fields such as dyeing, textile or packaging industry have been significantly gained. In this situation, the large scale of products has produced without any efficient inspection methods. It requires workers to detect manually by supervising the hundreds of meters of fabric or nylon. To avoid inconveniences or mistakes by human in manual operation, a novel idea to develop the automated inspection system is mentioned. The main architecture of this system comprises computational mechanics of several components, equipment placement and installation. Owing to the heavy load, two servo motors and chain drive are suggested to integrate in the driving mechanism. In this research, the principal factors to identify defect on surface are advanced techniques of computer vision. Several filters and image processing methods are implemented while the motion of rolls is executing. To validate our works, the real-world platform of proposed approach is entirely fulfilled. Some tests have been applied in this hardware in order to obtain the practical results. From these achievements, it could be obviously proved that our approach is feasible, efficient, and applicable for related industries.

1. Introduction

Our society is developing more and more since the industrialization and modernization are increasingly focused to enhance the level of each country, and improve citizen's living standards. Along with this process is the application of science and technology in areas of life such as health, technology, education, and social life [1]. Currently, several developers are trying to use many machines in automatic production stages, hence the number of products produced is increasing and fast. Product defect testing is an important aspect of modern industrial production [2]. The high cost of human-based inspection has led to the introduction of machine vision inspection devices.

In the industry of cloth or fabric, it is well-appeared in daily life as an convertible material. Textile fibers could be produced from natural components, for example cotton or wood [3], from combinations, i.e. wool, nylon or polyester [4]. For the mass production, human can not ensure the surface detection on fabric because any mistake is possibly ignored. Conventionally, in the approach of human inspection, these clothes are carried out in wooden board. Due to the fatigue or careless, fine detection is often unreachable. There is a need to deploy some

advanced techniques in order to assist in quality control. The automated inspections such as home textile fabric defect inspection machine system [5], visual two-stage inspection system [6] and computer-assisted system [7], become a natural trend forward to enhance the textile industry [8].

To deal with various targets, many investigators have studied different methods to detect. Developers in Ref. [9] has explored four types of defects detection of lumber by improving the feature fusion module of YOLOX. The benefits of this enhancement are to lessen the computational and parametric quantities as well as the speed and accuracy of wood defects detection. However, poor data set or limited model design could be the technical barriers for this method. For detecting defect on the tire surface [10–12], multi-texture background including the intra class dissimilarity and the inter class similarity becomes a challenging task. A novel end-to-end saliency detection network with hybrid loss function and coordinate attention module was invented. The possible application of this approach to deploy in the online visual detection is advantageous. Nevertheless, it might require an expert to adjust the network parameters. In the other development, a method consisting of a decoupled two-stage object detection framework

E-mail address: nhqthinh@hcmut.edu.vn.

¹ <https://doi.org/10.3991/ijxx.vx.ix.xxxx>.



Fig. 1. Conventional method for surface detection ^[a].

[a] <https://tetrainspection.com/>.

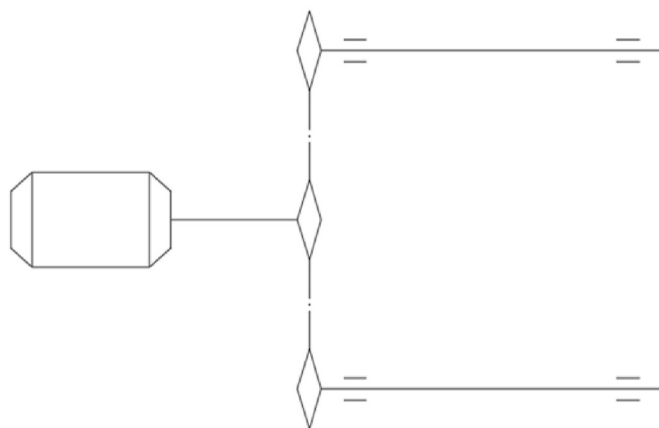


Fig. 2. Theoretical diagram for driving actuators.

based on convolutional neural networks, was presented for the surface defect detection of flexible printed circuit board [13]. Due to the diverse defects, multi-hierarchical aggregation block and non-local block were endorsed to locate feature and accurately classify similar defects. Although the detection accuracy through model pruning is reserved, the detection speed still needs to be boosted.

2. Literature review

To detect the faults in fabric as Fig. 1, there are many complicated factors to deal with the practical implementation. The contrast-based method between defects and fiber surface discovered that those regions with low contrast often led to misclassification [14]. They require the uniformly structured weaves and pre-determined feature fabrics. The arrangement in consistency of texture background also impacts on image acquisition owing to the color difference and distortion along a contextual scene [15]. In addition, the natures of defects including its size and shape, are the technical challenges in detection. It is critical to identify the defects of small size or recognize the gently similar pattern

[16]. The other factors from camera source such low resolution [17] or misalignment [18] of input image, cannot offer the exact characters of fabrics or wrong detection in template matching method. For the external devices and environmental conditions, the highly computational speed could prevent the delays in processing [19]. If the complexity of system increases, this speed in detection decreases proportionally. Lacking white light also delivers the poor results of detection [20]. It causes the improper illumination and low contrast.

As observed from numerous researches in related fields, scholars have performed their efforts to overcomes these drawbacks. There is no doubt that the proper methods depend on each characteristic of cloth, texture background or weaving method. To gain the satisfactory detection success rate, there is always a trade-off among many reasons in the design of defect detection methods, for instance machine performance, experienced practitioners, and the degree of success in automated inspection. Consequently, there are different solutions of automated inspection to adapt with those challenges. In statistical approach, various distributions of gray values consisting of auto-correlation function [21], co-occurrence matrix [22] and fractal dimension [23]. In the second approach, several transforms, i.e. Fourier transform [24], wavelet transform [25], Gabor transform [26] and filtering techniques [27], were used to eliminate sensitive noise and arduous disturbance. They could offer better response with small defects, but vulnerable to the on-board machinery vibration, electrical interference from machine. The other approaches need autoregressive model [28] or Markov random fields [29] for defect-free texture on fabric images.

3. Preliminaries

3.1. Computational mechanics

The fabric inspection system comprises one DC servo motor, two passively axes, metal chain for driving and gears as Fig. 2. This work requires to estimate the power of motor and shaft strength in the mechanical design. The design parameters of this system are initially setup with maximum speed 20 m/min, diameter of roll in full material 200 mm and without material 60 mm, the thickness of film 0.2 mm,

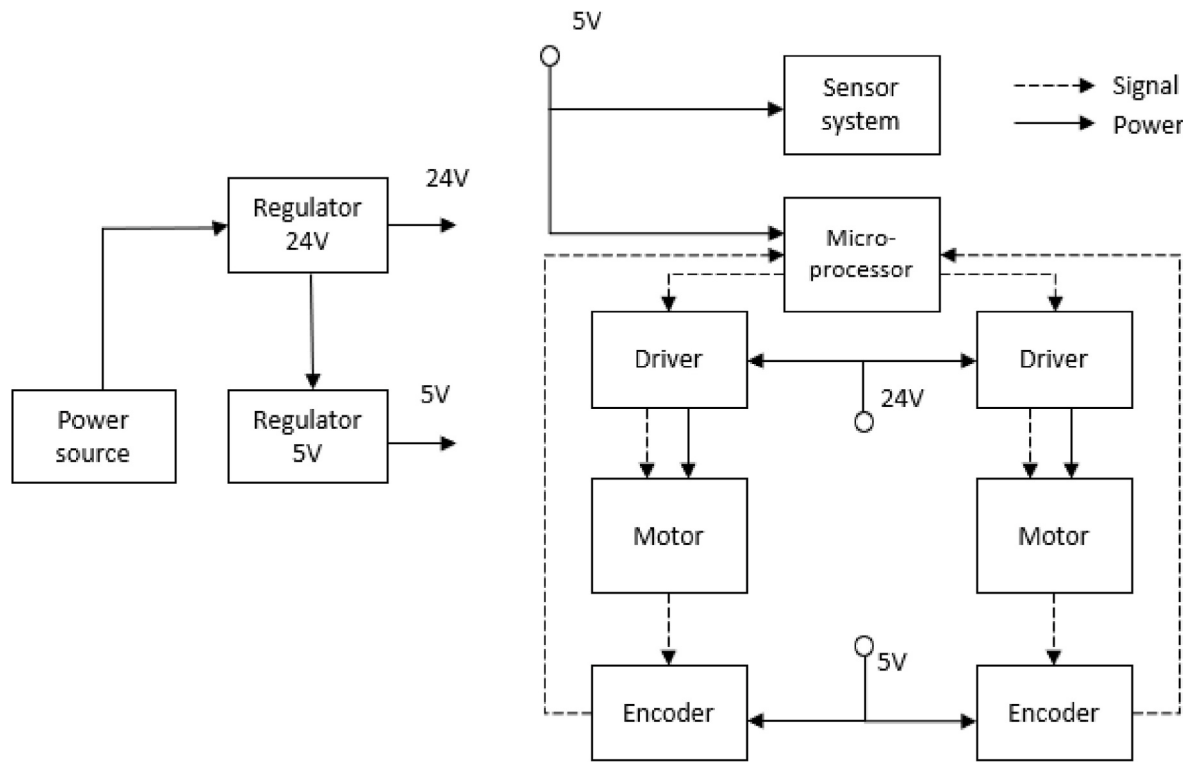


Fig. 3. Block diagram of electrical design.

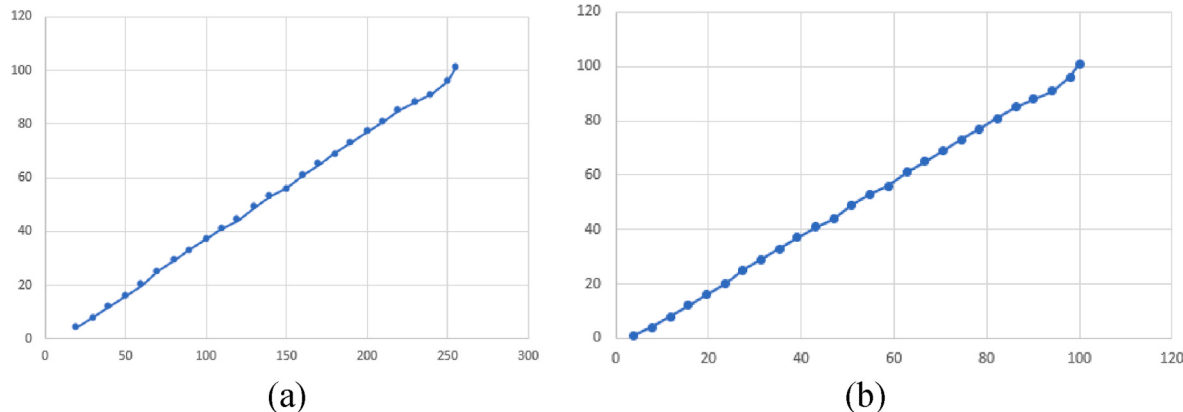


Fig. 4. Relationship performance between driver and right motor (a), left motor (b).

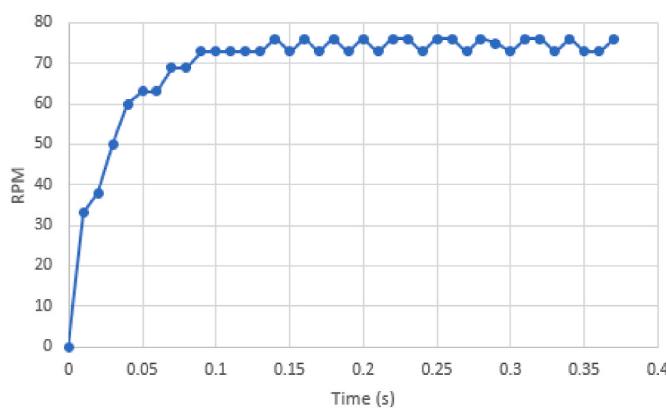


Fig. 5. Response of the driving motor with the step input.

maximum load 20 kg. The power to drive P_{ct} is identified as below,

$$P_{ct} = \frac{F \cdot v}{1000} = \frac{100 \cdot 0.333}{1000} = 0,033 \text{ (kW)} \quad (1)$$

where, F: force to drive.

v: velocity of roll.

This mechanism contains the driving chain and one bearing. The efficiency of driving mechanism is

$$\eta_{\Sigma} = \eta_x \cdot \eta_{ol}^2 \quad (2)$$

where, η_x : chain transmission efficiency, $\eta_x = 0,96$
 η_{ol} : bearing efficiency, $\eta_{ol} = 0,99$

$$\eta_{\Sigma} = 0,96 \cdot 0,99^2 = 0,941$$

Theoretically speaking, the power to drive P_{yc} is,

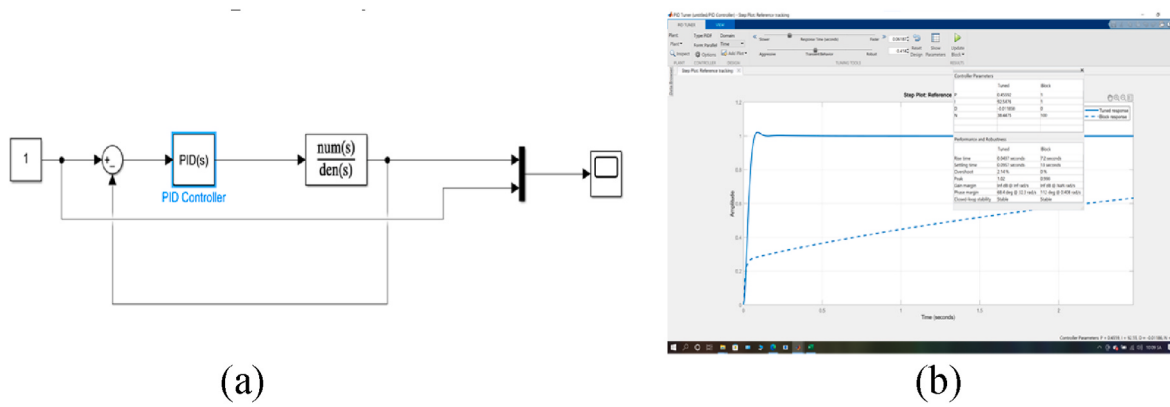


Fig. 6. Simulation of PID scheme using our model (a) and parameter estimation by PID Tuner Tool in Matlab (b).

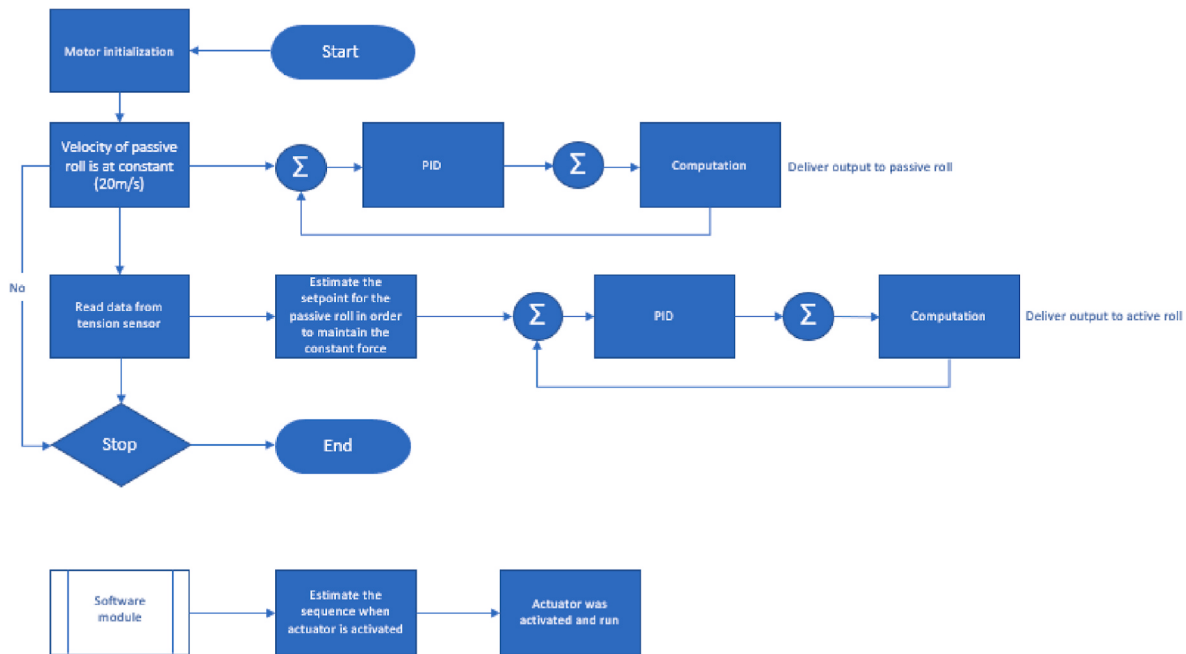


Fig. 7. Overview of the proposed approach.

$$P_{yc} = \frac{P_{ct}}{\eta_{\Sigma}} = \frac{0,033}{0,941} = 0,0167 \text{ (kW)} \quad (3)$$

To select the driving motor, some quantities must be evaluated firstly. The maximum velocity of active axis is,

$$n_{ct} = \frac{60000.v}{\pi.d} = \frac{60000.10.10^{-3}}{\pi.25} = 7,639 \text{ (round / min)} \quad (4)$$

where, v : velocity of belt conveyor, m/s

d : diameter of active axis, mm

The primary ratio should be estimated as below

$$n_{sb} = n_{ct}.u_{sb} = (7,639).1,6 = 12,223 \text{ (round / min)} \quad (5)$$

where, u_{sb} : coefficient of chain mechanism, according to our experience, this value is $u_{sb} = 1,6$

The moment on active axis is

$$T_m = 9,55.10^6 \cdot \frac{P_{ct}}{n_{ct}} = 9,55.10^6 \cdot \frac{0,0167}{7,639} = 20834,868 \text{ (Nm)} \quad (6)$$

Once, the specification of driving motor, i.e. power, velocity and moment, should be proper with our computations.

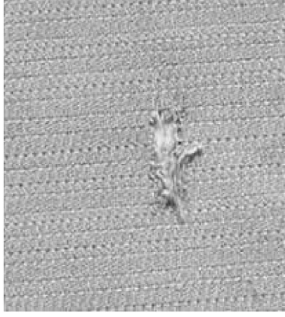
3.2. Electrical design

In Fig. 3, the electrical diagram uses centralized control technology with one microcontroller to manage all the tasks of the system. The system is divided into two main circuits. The central control circuit includes microcontroller blocks, driver blocks, 12 V, 5 V voltage stabilizers, and peripheral connectors. The sensing circuit consists of tension-measurement sensors. Power directly connects to the voltage regulator block of the central circuit to deliver in the other blocks of center circuit and also the sensor circuit. The driving motor and the external sensor circuit link to the central circuit to transmit signals to the microprocessor through connectors.

3.3. Sensor system

In this system, the sensing device comprises loadcell and positioning sensors. Usually, these sensors are attached directly to motor shaft in order to measure the system motion. Henceforward, loadcell plays a role as main source to estimate the tensions. The working principle is that the signal of output voltage is zero or close to zero when four resistors are matched in value. If there is a load or force acting on the loadcell body, it

Table 1
Some common defects on fabric surface.

Defect	Description	Reason
Perforation/ Hole		Caused by broken mechanical parts
Oil stains		Caused by oil on loom or other parts.
Torn		Caused by friction between fabric and sharp objects (mechanical part is broken)
Chipped thread/ Redundant only		Caused by thread tension causing excess thread break

is deformed (extended or compressed), leading to a change in the length and cross-section of the metal wires of the strain gage resistor. The result is to change output voltage. Sensor calibration by using the microcontroller to read the return value of a standard weight is essential. Then, it is correctly calibrated with that weight, and save the calibrating value for force calculation.

3.4. Modeling of drive motor

The driver selection becomes a crucial factor to possibly control the speed with high accuracy. It requires a driver that can respond quickly to high gain and remote driver poles. For our verification, the linear relationship between supply voltage (PWM-pulse width modulation through cycle duty) and motor speed is examined as Fig. 4. The increment in PWM in each time is 10, and the range is from 10 to 250. These signals input driver and read feed-back signals from positioning encoder.

The main power source that used for the driver is 24 V through the

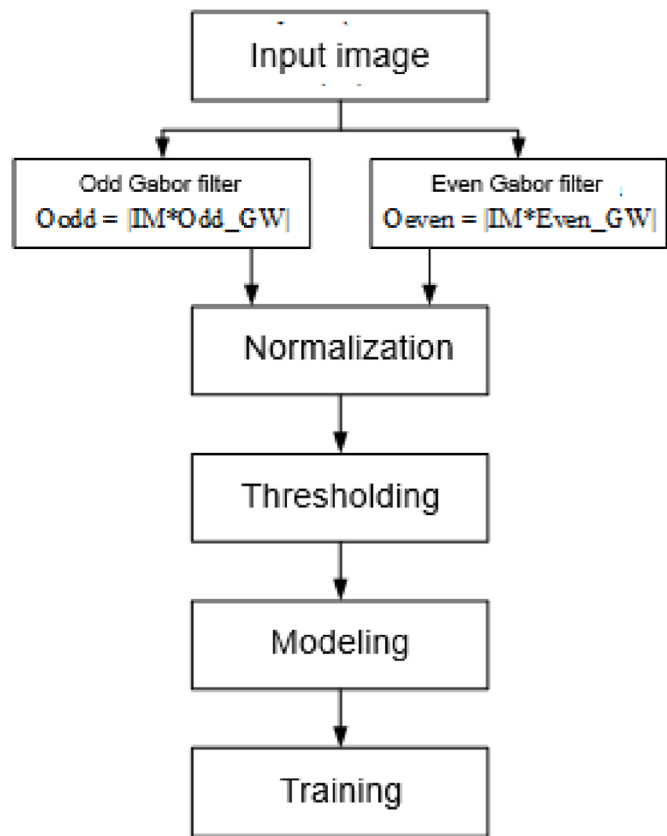


Fig. 8. Flowchart of the image processing validation in our approach.

voltage stabilizer block. At that moment, it is proceeded to adjust PWM with cycle duty 78% corresponding to the supply of 18.8 VDC to the motor. Due to the linearity that examined above of the driver, the transfer function of the driver block and the motor is found as Fig. 5. The PWM frequency is about 5 KHz to suppress the high frequency harmonics generated by the PWM wave to ensure the motor runs smoothly.

With these responses, in order to indicate the motion performance, the transfer function of driving motor is determined by System Identification Tool in Matlab as below,

$$\frac{12.8s - 2362}{s^2 + 1394s + 4.524e^4} \quad (7)$$

For better control of driving motor, the well-known PID scheme is deployed in our system. The benefits of this control scheme embrace simple structure, easy implementation and low computational cost. Additionally, the reason to choose this scheme is that the target of our investigation is to ensure the tracking performance as well as fast response. The key factor of PID control is to elect the proper coefficients in order to adapt with the driving results. To overcome the challenge, based on the above transfer function, it is simulated in Simulink/Matlab as Fig. 6. Far ahead, the output result of simulation is fed to PID Tuner Tool/Matlab which is aided to designate three parameters K_p , K_i and K_D respectively.

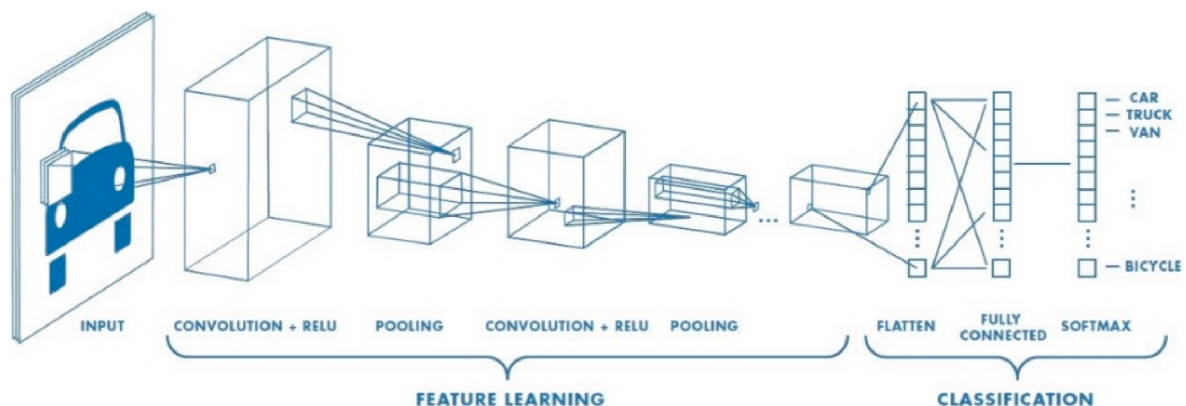
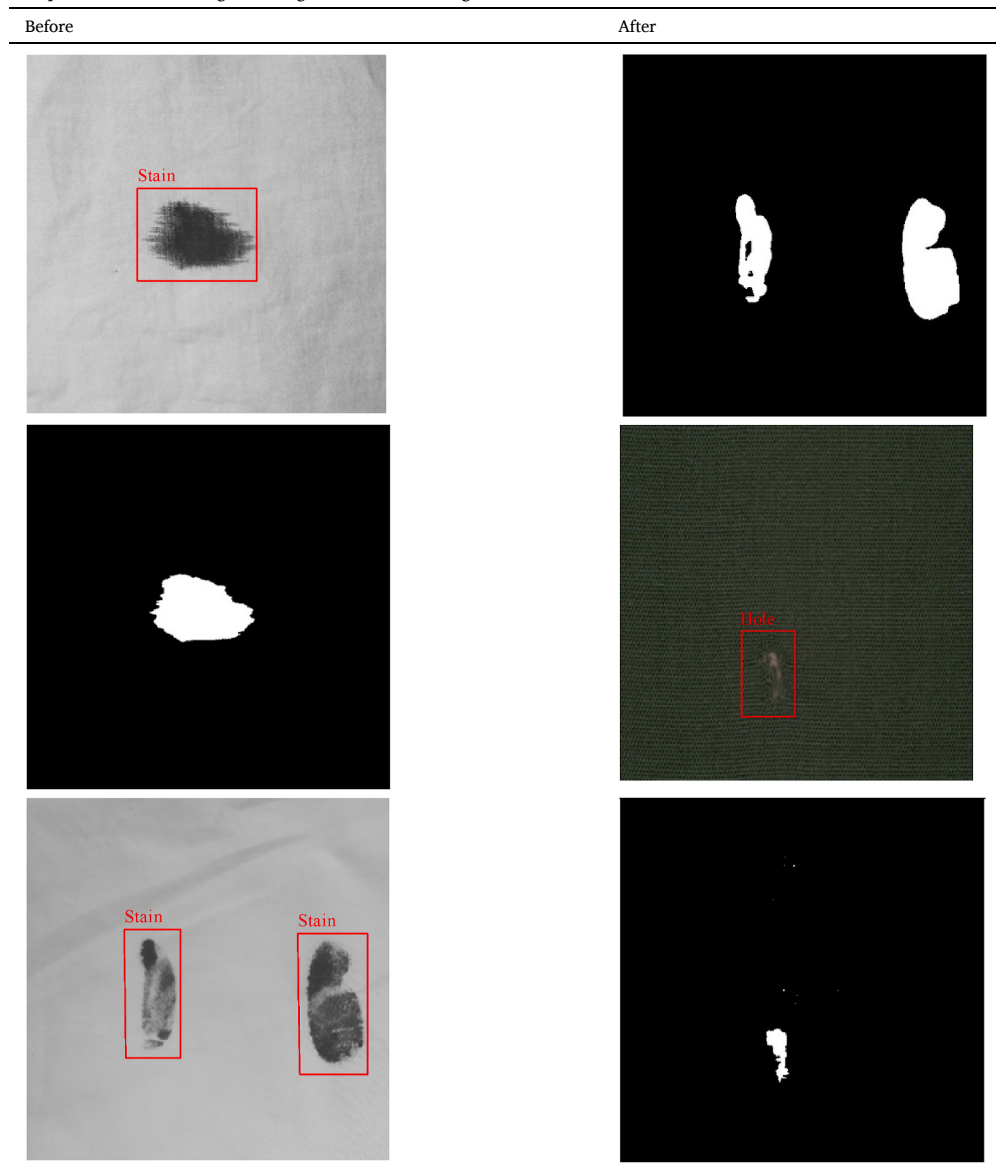
4. Proposed approach

4.1. Overall control scheme

To manipulate whole system, it is critical to drive the system logically. In that sense, the integration between control scheme and vision-based technique is introduced as Fig. 7. Because there are two rolls such roll forward and roll back, the control issue should contain two separate PID schemes for each. At initial stage, the same value of velocity is sent

Table 2

Comparison between original image and after filtering.

**Fig. 9.** Structure of a convolutional neural network (CNN)^[b].[b] <https://saturncloud.io/blog/a-comprehensive-guide-to-convolutional-neural-networks-the-eli5-way/>.

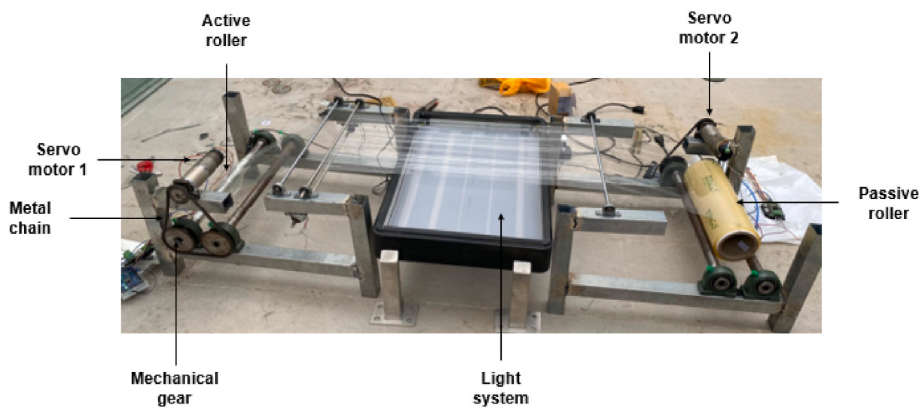


Fig. 10. Experimental set-up of our system.

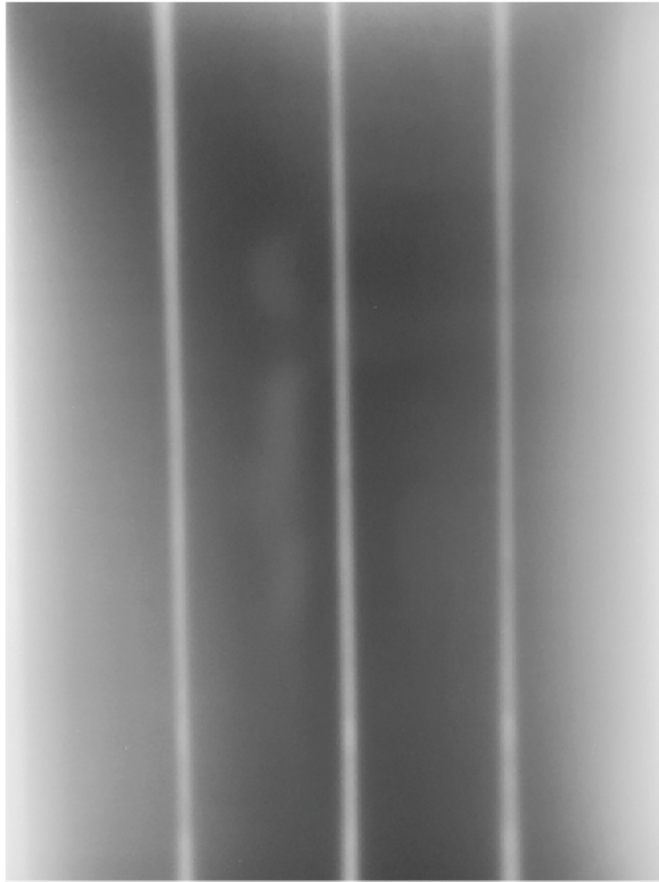


Fig. 11. Experimental result of camera capture for the proposed approach.

to both motors to produce the similar motion. The main micro-processor computes the driving commands in each sampling time and receives the feedback signal from sensors. Simultaneously, host computer which handles the image processing work, proceed to launch the visual computations. Due to the powerful abilities in mathematical solution, the vision-based results should be released on time. Throughout the driving procedure, the motor control is modified if there is any trouble in the image processing work.

4.2. Vision-based techniques

In the fabric industry, many manufacturers make their efforts to produce the high-quality products. However, defects still exist on the

fabric surface. It is important to note that these defects can vary in severity, from minor imperfections that may go unnoticed to more significant flaws that affect the fabric's functionality and aesthetic appeal. As [Table 1](#), the classification of typical defects is described and its reasons.

The framework of proposed system to detect the surface defect consists of several stages which are pre-processing, filtering and normalization, thresholding, modeling, and training, and detecting as [Fig. 8](#). The role of pre-processing technique is to re-arrange the raw data after capturing in outdoor environment. In the filtering step, two digital filters are suggested to refine this data. The gaussian filter is to regularize image data while maintaining model accuracy. It is a widely used effect in graphics software, typically to reduce image noise and reduce detail. The visual effect of this blurring technique is a smooth blur resembling that of viewing the image through a translucent screen, distinctly different from the bokeh effect produced by an out-of-focus lens or the shadow of an object under usual illumination. Secondly, median filter which is a non-linear digital filtering technique, often used to remove noise from an image or signal. Such noise reduction is a typical pre-processing step to improve the results of later processing (for example, edge detection on an image). Median filtering is very widely used in digital image processing because, under certain conditions, it preserves edges while removing noise (but see the discussion below), also having applications in signal processing.

Theoretically speaking, the purpose of dynamic range expansion in the various applications is usually to bring the image, or other type of signal, into a range that is more familiar or normal to the senses, hence the term normalization. Often, the motivation is to achieve consistency in dynamic range for a set of data, signals, or images to avoid mental distraction or fatigue. Hence, normalization is a process that changes the range of pixel intensity values as [Table 2](#). Applications include photographs with poor contrast due to glare. Normalization is sometimes called contrast stretching or histogram stretching. In digital image processing, thresholding is the simplest method of segmenting images. From a grayscale image, thresholding can be used to create binary images.

The loss value represents the difference between the predicted value and the true value in the training process and detection. Also, the size of this value inversely relates to the recognition effect of the predicted box. The model in our investigation outperforms in high precision and rapid processing. In next section, the experimental tests that indicate these values of loss function, would be portrayed.

Although the result of gabor filter is rather good, some cases still exist noise or wrong detection. Thus, it is essential to implement an additional stage to verify such CNN-based method. In fact, a CNN network as [Fig. 9](#) is a collection of convolution layers that overlap and use nonlinear activation functions like ReLU and tanh to activate the weights in the nodes. Each layer, after being activated, can generate more abstract

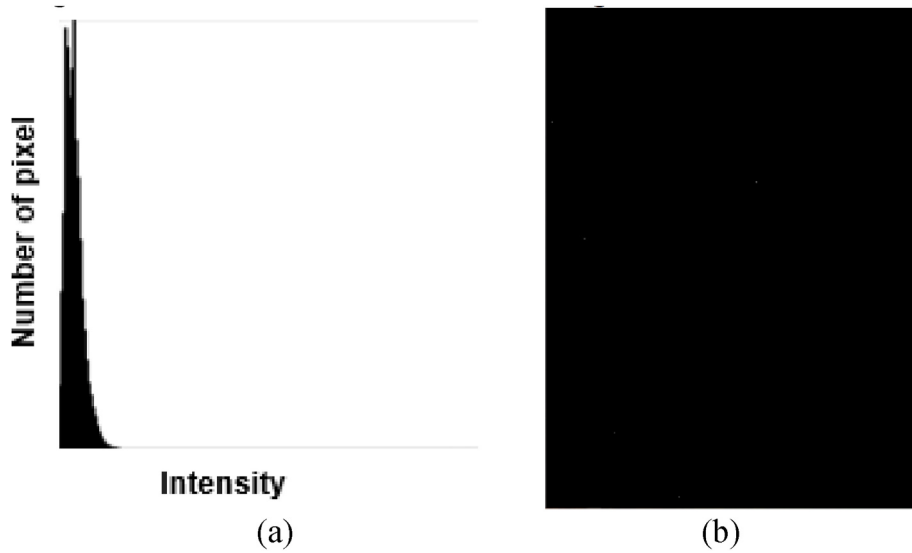


Fig. 12. Experimental result of histogram (a) and experimental result of thresholding work for the proposed approach (b).

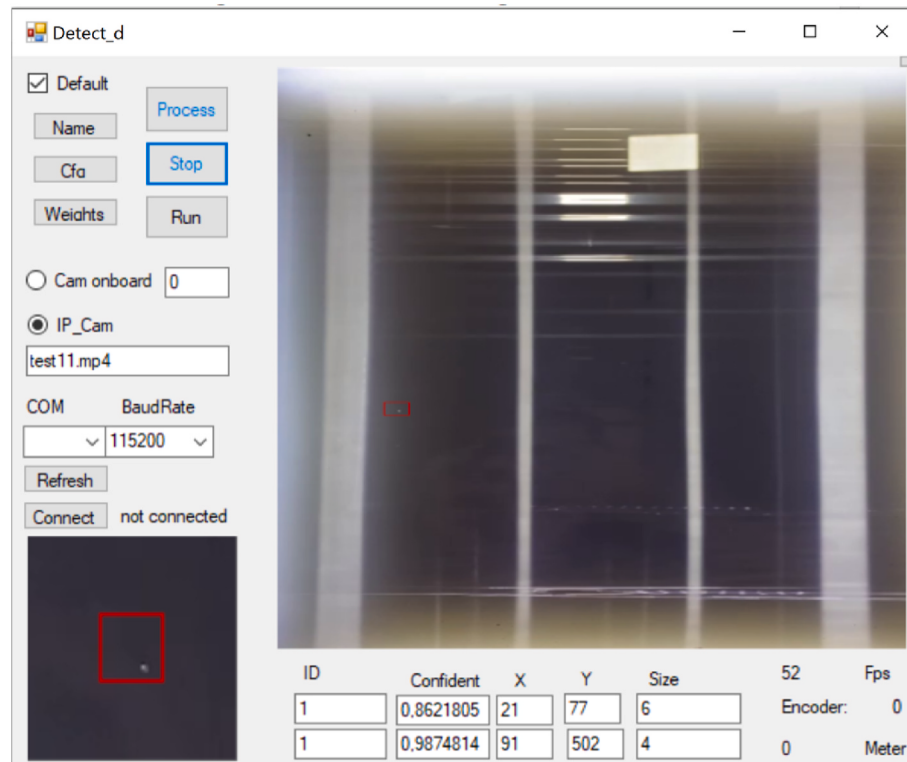


Fig. 13. Experimental result of software development for the proposed approach.

information for the next layers.

The basic structure of CNN has three main parts:

- Location receptive fields: help to filter out the information of the image and select the most valuable image areas.
- Shared weights and bias: reduce the maximum number of weights and the number of parameters in the CNN.
- Pooling layer: simplifies the output information to get the most easy-to-use results.

In the CNN model, there are two properties that need attention: location invariance and coherence or compositionality. With the same

object, if projected from different angles (translation, rotation, scaling), accuracy would be significantly affected.

Pooling layer would show invariance to translation, rotation, and scaling. Local associativity gives lower-to-higher and more abstract levels of information representation through convolution from filters. That is why CNN produces a model with very high accuracy. Therefore, our design comprises 53 convolution layers connecting in series. These layers are responsible for detecting objects with up to 106 layers. The output would be a vector including

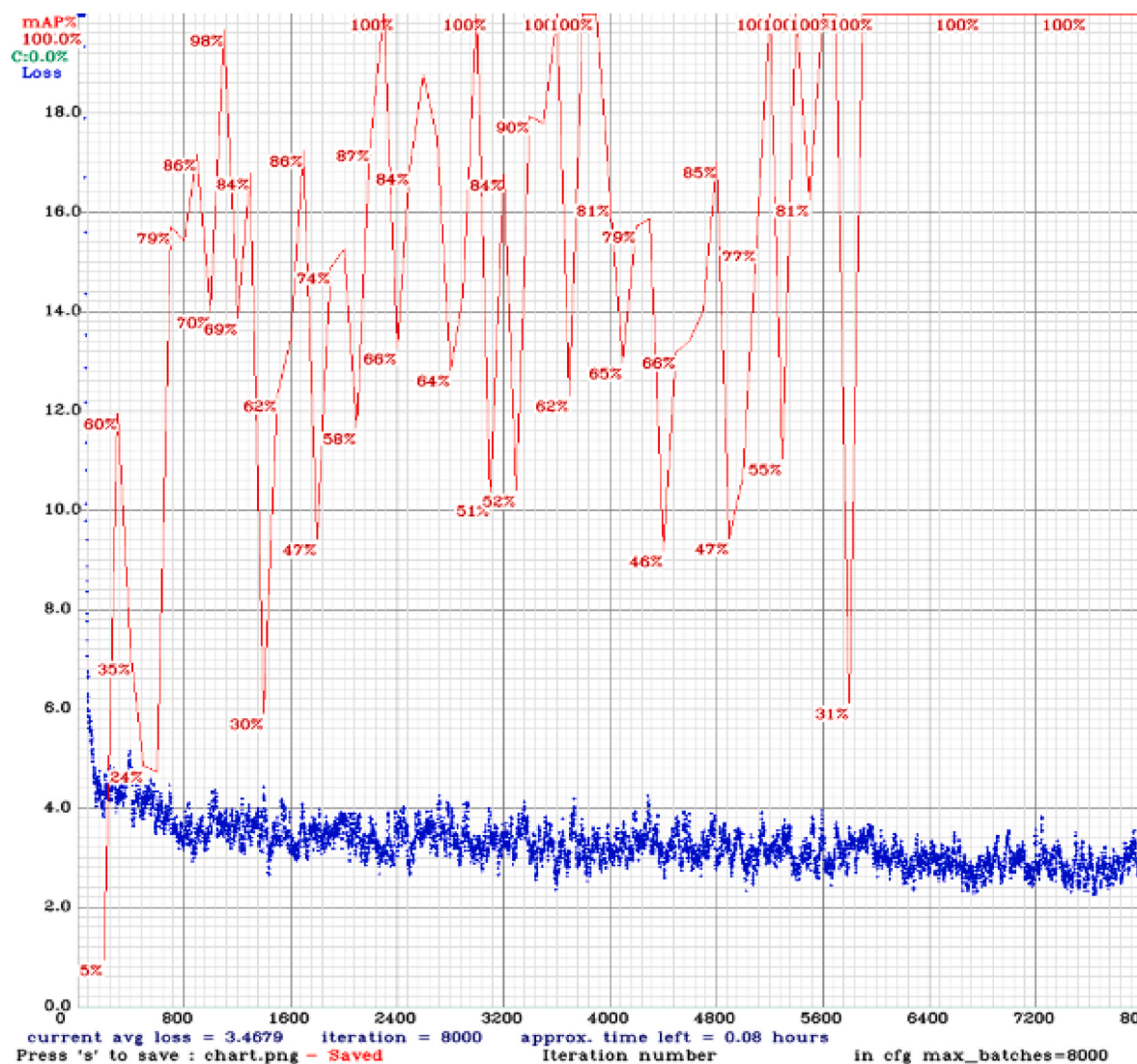


Fig. 14. Experimental result of thresholding work for the proposed approach.

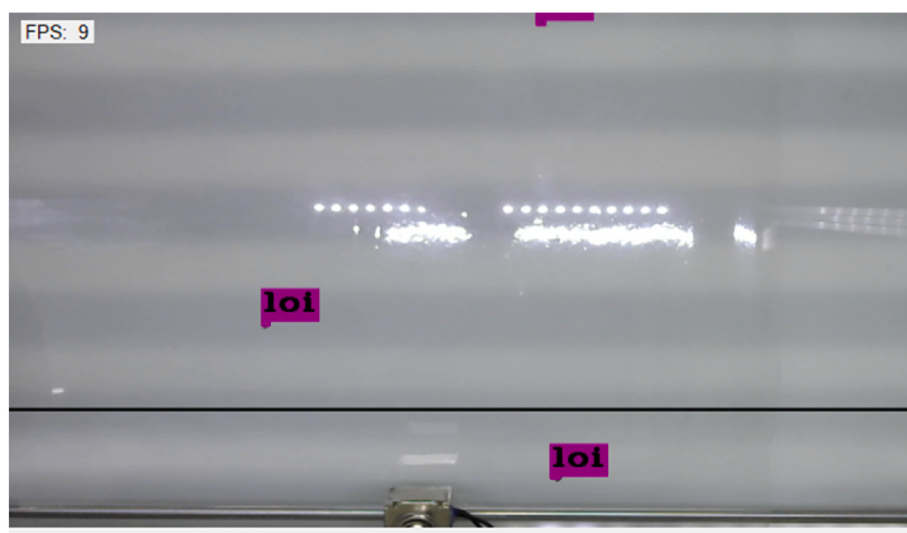


Fig. 15. Experimental result of defect detections for the proposed approach.

Table 3

Statistics of the results of counting the number of defects on the surface.

Speed	Time (min)	Number of detected defects	Precision	Average Precision	Frame per second (Fps)
v = 2 cm/s	5	47/50	94%	92,8%	6-14 fps
v = 4 cm/s	2,7	47/50	94%	92,5%	
v = 6 cm/s	2	46/50	92%	91,1%	
v = 8 cm/s	1,25	43/50	86%	84,7%	

$$\mathbf{y}^T = \left[p_0, \underbrace{\langle t_x, t_y, t_w, t_h \rangle}_{\text{bounding box}}, \underbrace{\langle p_1, p_2, \dots, p_c \rangle}_{\text{scores of } c \text{ classes}} \right] \quad (8)$$

where,

- p_0 – predicted probability of the object appearing in the bounding box.
- $\langle t_x, t_y, t_w, t_h \rangle$ – to identify the bounding box. t_x, t_y are coordinate of center and t_w, t_h are dimensions (length, width) of the bounding box.
- $\langle p_1, p_2, \dots, p_c \rangle$ – vector for probability distribution of classes.

5. Laboratory results

To verify the proposed approach, the real-world hardware is launched due to our design. Firstly, the mechanical parts and basement are produced to link two rolls. It must be able to sustain heavy load because the roll of cloth or nylon roll is rather weighty. In the initial stage, active roller with empty load provides greater moment to drive firstly. Then, passive roller which carry load, is driven behind. After that, the driving mechanism is attached into this platform while the control board is connected to host computer. Driving actuators consist of long metal chain, mechanical gears, and axial rollers. Two DC servo motors are utilized to directly drive both rolls. The light system is in the middle of this inspection system. In this section, quantitative tests are implemented to extract defect feature automatically with high accuracy on detection as Fig. 10.

Initially, host computer would check the system state including the status of motor, camera and driving mechanism. Subsequently, in the pre-processing stage, it focuses on extracting the area that is likely to contain product errors and extracting a window to that container to reduce the computational volume. This data from camera capture as Fig. 11, is converted to gray image. Then, it is the input source for next stage where the filtering techniques are deployed. With the effects of two digital filters, data image is to make regular and remove noise from surrounding.

The next stage is to normalize image in order to keep changing the range of pixel intensity values. Since the contrast of picture might be poor in some cases, it is necessary to achieve consistency in dynamic range for a set of data. The result of histogram after subtracting is

illustrated as Fig. 12a.

Since then, for each pixel in image, bias value is compared to ensure that there is no significant difference. Consequently, in most methods, the same threshold is applied to all the pixel of an image. However, in some cases, it can be advantageous to apply a different threshold to different parts of the image, based on the local value of the pixels. This category of methods is called local or adaptive thresholding. They are particularly adapted to cases where images have inhomogeneous lighting. As a result, this method is applied in this investigation as Fig. 12b.

To launch a model which is able to detect the defect surface, it requires several following steps. From some experts and experiences, the dataset should be collected in large scale firstly. The common errors in product such scratch, puncture or unregular distribution of materials, are expected to screen. These images are fed to computer in order to convert to gray data, labelling, trim to 128×128 window. With high power of GPU (Graphics Processing Unit), the training process is done in local computer. To halt this procedure, the condition for loss function must be reached [30]. Currently, the training results return some specifications, for instance weights, configs, and names. For the following applications, each frame of image is recognized via API functions (Application Programming Interface). The structure of convolution neural network includes 23 convolution layers, interspersed with max-pool layers. Activation functions are leaky Relu and linear whilst there are two classes with input size 128×128 . In host computer, the GUI (Graphical User Interface) program is built as Fig. 13. With Windows 10 operating system, CUDA 10.0, OpenCV 2.4, it is expected to proceed this work completely. Some indicators of the proposed system are demonstrated as Fig. 14. It is clearly seen that all parameters specify the well-adapted performance in our tests.

By using the open-source libraries such OpenCV, it is explored more functions for the image processing techniques. In computer vision, blob detection methods are aimed at detecting regions in a digital image that differ in properties, such as brightness or color, compared to surrounding regions. Informally, a blob is a region of an image in which some properties are constant or approximately constant; all the points in a blob can be considered in some sense to be like each other. After classifying the regions and identify the coordinate of center points, a window which has the same size with inputs of model, is extracted. If there exist blobs in the same window, then it is merged and the center of window is the midpoint between two centers. The real-world result of defect detections by using our method is represented as Fig. 15. For the setting conditions, these tests are verified with 9 frames per second, vertical view, and single camera. To evaluate the precision of the defect detection algorithm, dataset is collected and labelled so that 80% of its is utilized for training and 20% of its is for validating. The ratio of Intersection over Union (IoU) is recommended to discuss as below,

$$IoU = \frac{\text{area}(B_p \cap B_{gt})}{\text{area}(B_p \cup B_{gt})} \quad (9)$$

where,

 B_p : area of image where the model predicts the objects B_{gt} : area of image where contains the objects (labelled data).

The precision of our detection is measured by

Table 4

List of comparative experiments between our approach and the others.

Method	Network structure	Light source	Proposed model	Purpose of study	Texture
Our approach	Four layers with feature extraction	Multi LEDs	CNN-based method	Fusion between mechanics, electrics, and vision	Reflective or non-reflective surface fabrics with different contrasts
Zhang, K. et al. [32]	N/A	N/A	Color-based method	Using the color dissimilarity and the positional aggregation	The motif and box-patterned fabrics
Chakraborty, S. et al. [31]	Multi-layer with image classification	Not explicitly mentioned	CNN-based method	Model with newly added dropout and global average pooling layer	Printed fabrics

N/A: not applied.

$$precision = \frac{TP}{TP + FP} \quad (10)$$

where,

True positive (TP): model correctly recognizes object class with $IoU \geq 0, 5$.

False positive (FP): the model cannot recognize the object properly or recognize it properly but $IoU < 0, 5$.

Besides, the average precision (AP) is also mentioned as

$$p_{interp}(r) = max_{r' \geq r} p(r') \quad (11)$$

$$AP = \sum_{i=1}^{n-1} (r_{i+1} - r_i) p_{interp}(r_i + 1) \quad (12)$$

In the second verification, one roll is prepared with a known number of errors (50 errors). Host computer would drive the receiver roll at different speeds of 2, 4, 6, 8 cm/s and the videos are recorded. The software program executes our algorithm and return the number of defects that it detects. From these cases, the results in Table 3 are obtained.

Above table presents the defect count results. Experimental validations show that the average precision which is measured on four video data, is achieved. It was observed that the defects in this algorithm mainly occurred in the frames containing the defects located too close together. The processing speed of system including the recognition and counting, falls in the range of 6–14 fps. Obviously, it depends on the size of the image margin and the number of defects in a frame.

To conduct the competitive performance between our method and the other methods, Table 4 provides several comparisons in each category. It is noted that these researches are completed in recent years in order to ensure the up-to-date technique. For the topic of inspection system, there is a trend to investigate on the convolutional neural network such [31]. Also, the typical approach using color-based segmentation is denoted as [32]. The objective targets could be varied according to the technical specifications of quality of image, computer vision or hardware design.

6. Conclusion

In this paper, an efficient solution for the automated inspection system was presented. Both theoretical computations and simulations in mechanics, electrics and control scheme were discussed and evaluated. There are several advanced techniques which were integrated in the vision-based approach. Owing to this implementation, the system performance could be enhanced and more superior. The benefits of our works are to innovate the low-cost platform, open-source mechanism, and outperform in many experimental validations. From these results, it would be considered evidently that this method is feasible and applicable to inspect defect in many fields.

Credit author statement

Ha Quang Thinh Ngo: Conceptualization, Methodology, Software, Writing- Reviewing and Editing Ha Quang Thinh Ngo: Data curation, Writing- Original draft preparation. Ha Quang Thinh Ngo: Visualization, Investigation, Supervision.

Declaration of competing interest

The authors declare that they have no known competing financial interests or personal relationships that could have appeared to influence the work reported in this paper.

Data availability

Data will be made available on request.

Acknowledgement

We acknowledge Ho Chi Minh City University of Technology (HCMUT), VNU-HCM for supporting this study.

References

- [1] A. Rasheed, B. Zafar, A. Rasheed, N. Ali, M. Sajid, S.H. Dar, M.T. Mahmood, Fabric defect detection using computer vision techniques: a comprehensive review, *Math. Probl. Eng.* 2020 (2020).
- [2] N.C. Sandhya, N.M. Sashikumar, M. Priyanka, S. Maria, K.K. Wenisch, Automated fabric defect detection and classification: a deep learning approach, *Textile & Leather Review* 4 (2021) 315–335.
- [3] N. Amor, M.T. Noman, M. Petru, Classification of textile polymer composites: recent trends and challenges, *Polymers* 13 (16) (2021) 2592.
- [4] Y. Chen, Y. Ding, F. Zhao, E. Zhang, Z. Wu, L. Shao, Surface defect detection methods for industrial products: a review, *Appl. Sci.* 11 (16) (2021) 7657.
- [5] J. Barman, H.C. Wu, C.F.J. Kuo, Development of a real-time home textile fabric defect inspection machine system for the textile industry, *Textil. Res. J.* (2022), 00405175221111477.
- [6] V. Voronin, R. Sizyakin, M. Zhdanova, E. Semenishchev, D. Bezuglov, A. Zelemskii, June. Automated visual inspection of fabric image using deep learning approach for defect detection, in: *Automated Visual Inspection and Machine Vision IV*, vol. 11787, SPIE, 2021, pp. 174–180.
- [7] P.R. Jeyaraj, E.R.S. Nadar, Effective textile quality processing and an accurate inspection system using the advanced deep learning technique, *Textil. Res. J.* 90 (9–10) (2020) 971–980.
- [8] H.Y. Ngan, G.K. Pang, N.H. Yung, Automated fabric defect detection—a review, *Image Vis. Comput.* 29 (7) (2011) 442–458.
- [9] D. Li, Z. Zhang, B. Wang, C. Yang, L. Deng, Detection method of timber defects based on target detection algorithm, *Measurement* 203 (2022), 111937.
- [10] Z. Zheng, H. Yang, L. Zhou, B. Yu, Y. Zhang, HLU 2-Net: a residual U-structure embedded U-Net with hybrid loss for tire defect inspection, *IEEE Trans. Instrum. Meas.* 70 (2021) 1–11.
- [11] Y. Zhang, D. Lefebvre, Q. Li, Automatic detection of defects in tire radiographic images, *IEEE Trans. Autom. Sci. Eng.* 14 (3) (2015) 1378–1386.
- [12] M. Zhao, Z. Zheng, Y. Sun, Y. Chang, C. Tian, Y. Zhang, MSA-Net: efficient detection of tire defects in radiographic images, *Meas. Sci. Technol.* 33 (12) (2022), 125401.
- [13] J. Luo, Z. Yang, S. Li, Y. Wu, FPCB surface defect detection: a decoupled two-stage object detection framework, *IEEE Trans. Instrum. Meas.* 70 (2021) 1–11.
- [14] L. Bissi, G. Baruffa, P. Placidi, E. Ricci, A. Scorzoni, P. Valigi, Automated defect detection in uniform and structured fabrics using Gabor filters and PCA, *J. Vis. Commun. Image Represent.* 24 (7) (2013) 838–845.
- [15] W. Ouyang, B. Xu, J. Hou, X. Yuan, Fabric defect detection using activation layer embedded convolutional neural network, *IEEE Access* 7 (2019) 70130–70140.
- [16] L. Liu, J. Zhang, X. Fu, L. Liu, Q. Huang, Unsupervised segmentation and elm for fabric defect image classification, *Multimed. Tool. Appl.* 78 (9) (2019) 12421–12449.
- [17] G.H. Hu, Q.H. Wang, Fabric defect detection via un-decimated wavelet decomposition and gumbel distribution model, *Journal of Engineered Fibers and Fabrics* 13 (1) (2018), 155892501801300103.
- [18] J.K. Park, W.H. An, D.J. Kang, Convolutional neural network based surface inspection system for non-patterned welding defects, *Int. J. Precis. Eng. Manuf.* 20 (3) (2019) 363–374.
- [19] D. Peng, G. Zhong, Z. Rao, T. Shen, Y. Chang, M. Wang, June. A fast detection scheme for original fabric based on Blob, canny and rotating integral algorithm, in: 2018 IEEE 3rd International Conference on Image, Vision and Computing (ICIVC), IEEE, 2018, pp. 113–118.
- [20] C. Panigrahy, A. Seal, N.K. Mahato, D. Bhattacharjee, Differential box counting methods for estimating fractal dimension of gray-scale images: a survey, *Chaos, Solitons & Fractals* 126 (2019) 178–202.
- [21] X.Y. Zhang, C.L. Liu, C.Y. Suen, Towards robust pattern recognition: a review, *Proc. IEEE* 108 (6) (2020) 894–922.
- [22] O.I. Abiodun, A. Jantan, A.E. Omolara, K.V. Dada, A.M. Umar, O.U. Linus, M. U. Kiru, Comprehensive review of artificial neural network applications to pattern recognition, *IEEE Access* 7 (2019) 158820–158846.
- [23] J.E. Park, S.Y. Park, H.J. Kim, H.S. Kim, Reproducibility and generalizability in radiomics modeling: possible strategies in radiologic and statistical perspectives, *Korean J. Radiol.* 20 (7) (2019) 1124–1137.
- [24] J. Xiang, R. Pan, W. Gao, Yarn-dyed Fabric Defect Detection Based on an Improved Autoencoder with Fourier Convolution, *Textile Research Journal*, 2022, 00405175221130519.
- [25] G.H. Hu, Q.H. Wang, Fabric defect detection via un-decimated wavelet decomposition and gumbel distribution model, *Journal of Engineered Fibers and Fabrics* 13 (1) (2018), 155892501801300103.
- [26] M. Chen, L. Yu, C. Zhi, R. Sun, S. Zhu, Z. Gao, Y. Zhang, Improved faster R-CNN for fabric defect detection based on Gabor filter with Genetic Algorithm optimization, *Comput. Ind.* 134 (2022), 103551.

- [27] S. Vargas, M.E. Stivanello, M.L. Roloff, É. Stiegelmaier, M.R. Stemmer, Development of an online automated fabric inspection system, *Journal of Control, Automation and Electrical Systems* 31 (1) (2020) 73–83.
- [28] L. Jia, C. Chen, S. Xu, J. Shen, Fabric defect inspection based on lattice segmentation and template statistics, *Inf. Sci.* 512 (2020) 964–984.
- [29] Y. Shi, Y. Gao, Y. Zhang, J. Sun, X. Mou, Z. Liang, Spectral CT reconstruction via low-rank representation and region-specific texture preserving Markov random field regularization, *IEEE Trans. Med. Imag.* 39 (10) (2020) 2996–3007.
- [30] J. Redmon, S. Divvala, R. Girshick, A. Farhadi, You only look once: unified, real-time object detection, in: *Proceedings of the IEEE Conference on Computer Vision and Pattern Recognition*, 2016, pp. 779–788.
- [31] S. Chakraborty, M. Moore, L. Parrillo-Chapman, June), Automatic printed fabric defect detection based on image classification using modified VGG network, in: *International Conference on Applied Human Factors and Ergonomics*, Springer International Publishing, Cham, 2021, pp. 384–393.
- [32] K. Zhang, Y. Yan, P. Li, J. Jing, X. Liu, Z. Wang, Fabric defect detection using salience metric for color dissimilarity and positional aggregation, *IEEE Access* 6 (2018) 49170–49181.